

Technical Notes

Multi-Objective Optimization of Rocket-Based Combined-Cycle Engine Performance Using a Hybrid Evolutionary Algorithm

Dario Pastrone* and Matteo Rosa Sentinella†
Politecnico di Torino, 10129 Turin, Italy

DOI: 10.2514/1.41327

Nomenclature

A	=	ejector-mixing-duct area
A^*	=	rocket throat area
c^*	=	rocket characteristic velocity
I_s	=	specific impulse
\mathcal{M}	=	molecular mass
M	=	Mach number
\dot{m}	=	mass flow rate
p	=	pressure
T	=	temperature
T	=	thrust
T/A	=	thrust to area ratio
u	=	flight speed
w	=	velocity
\mathbf{x}	=	design parameters vector
α	=	ejector-to-primary-nozzle-throat area ratio
β	=	primary-to-secondary total pressure ratio
β_n	=	nozzle expansion ratio
γ	=	specific heat ratio
δ	=	ramjet-fuel-to-primary mass flow rate
ε	=	nozzle area ratio
μ	=	secondary-to-primary mass flow rate
ν	=	primary-to-secondary molecular mass ratio
ν_3	=	mixed-to-secondary molecular mass ratio
τ	=	primary-to-secondary total temperature ratio
τ_3	=	mixed-to-secondary total temperature ratio
Φ	=	overall equivalence ratio
φ	=	rocket chamber mixture ratio
χ	=	ejector operation parameter

Subscripts

ck	=	secondary-flow choking
e	=	engine exit
$M3$	=	ejector-exit choking
p	=	primary flow

s	=	secondary flow
0	=	upstream/ambient
$1, 3, 7$	=	engine stations, see Fig. 1

Superscript

o	=	total
-----	---	-------

I. Introduction

ROCKET-BASED combined-cycle (RBCC) engines promise low-cost space access. They combine airbreathing and rocket propulsion elements into a single integrated engine which is capable of multimode operation and can be used from ground takeoff up to space. In this study a RBCC engine called an ejector-ram-rocket (ERR) engine is considered. In such an engine (Fig. 1) a rocket is used as the primary of an ejector from static conditions up to about Mach 2 or 3 to augment the pure ramjet thrust. At higher flight Mach numbers the rocket is shut off and the engine is operated as a ramjet. The same rocket is then reignited and used alone when the flight Mach number exceeds 6. This kind of engine presents interesting features, because it provides good thrust augmentation at low speeds while having mechanical simplicity [1]. When the flight Mach number is above sonic conditions the engine operates in ram rocket or air augmented rocket mode: The air entering the engine is determined by flight Mach number and inlet geometry, unless the engine determines subcritical/unstarted inlet conditions. On the other hand, at low flight Mach numbers, the engine is said to be operating in ejector rocket mode because the amount of air being entrained into the engine depends on numerous factors within the ejector itself and the evaluation of the flowfield results to be more intriguing. Moreover, at low flight speeds the dynamic pressure is low and high thrust to area ratio must be obtained with affordable propellant consumption: A multi-objective optimization problem should be solved, considering both thrust to area ratio and specific impulse.

A large number of works concerning numerical and experimental RBCC engine investigation can be found in the literature [2]. Some works focus on ejector performance such as entrained air and total pressure ratio [3,4]. Even if some authors consider the effects due to molecular weight [5], other ejector performance parameters that influence thrust augmentation, such as the total temperature and specific heat of the flow exiting the engine, are not usually considered. The best is to consider thrust as compared to propellant consumption and engine size. Parametric studies can be found which investigate ejector thrust augmentation [6]. Jahingir and Huque [7] used computational fluid dynamics modeling and neural network to search for the ejector design variables that maximize a desirability function which includes bypass ratio, compression ratio, and ejector nozzle efficiency.

The present study goal is to develop and demonstrate a multi-objective design optimization method for RBCC engines. Discontinuous or concave Pareto fronts can be a real concern for mathematical programming techniques. Therefore, a method based on evolutionary algorithms (EAs) has been developed and proved. Because the model used to evaluate the ejector's performance will be recalled several times by the optimization procedures, a control-volume approach is used, similar to those used by other authors [4,5,8–10], in order to have a reasonable computation time. With respect to previous studies the model is here improved. The effects of the gas properties, which depend on the primary rocket propellant combination and mixture ratio and on the ramjet equivalence ratio, are taken into account. Moreover, the ejector operation constraints are properly highlighted.

Presented as Paper 5170 at the 44th AIAA/ASME/SAE/ASEE Joint Propulsion Conference and Exhibit, Hartford, CT, 21–23 July 2008; received 30 September 2008; revision received 26 May 2009; accepted for publication 26 May 2009. Copyright © 2009 by the American Institute of Aeronautics and Astronautics, Inc. All rights reserved. Copies of this paper may be made for personal or internal use, on condition that the copier pay the \$10.00 per-copy fee to the Copyright Clearance Center, Inc., 222 Rosewood Drive, Danvers, MA 01923; include the code 0748-4658/09 and \$10.00 in correspondence with the CCC.

*Associate Professor, Dipartimento di Energetica, Corso Duca degli Abruzzi, 24. Senior Member AIAA.

†Research Assistant, Dipartimento di Energetica, Corso Duca degli Abruzzi, 24.

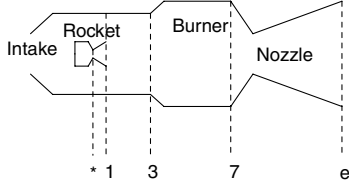


Fig. 1 Schematic of the ERR engine.

II. Statement of the Problem and Modeling

The optimization objectives are the specific impulse I_s and thrust to ejector-mixing-duct area ratio T/A . An optimum expansion is assumed ($p_e = p_0$), then

$$I_s = \frac{(1 + \mu + \delta)w_e - \mu u}{g_0(1 + \delta)}; \quad T/A = \frac{g_0(1 + \delta)I_s p_p^o}{c^* \alpha} \quad (1)$$

The exit velocity w_e can be evaluated

$$w_e = \sqrt{2c_{pe}T_e^o(1 - \beta_n^{\frac{1-\gamma_e}{\gamma_e}})} \quad (2)$$

by using proper mean values of c_{pe} and γ_e , here evaluated by a code subroutine validated by a comparison with CEA code [11]. For a given flight condition, the performance depends on the ramjet-fuel mass flow and on the operating conditions of the ejector.

A. Ejector Modeling

It is assumed that the throat area A^* of the primary rocket nozzle is choked and that a supersonic primary flow entrains a subsonic secondary flow into a constant-area ejector mixing duct. The conservation equations (continuity, momentum, and energy) are applied to the overall control volume consisting of the constant-area ejector mixing duct. A frictionless, steady, adiabatic flow is assumed, neglecting pressure losses due to air intake compression, primary-/secondary-flow interaction, heat release, and flame holders. Uniform velocity and pressure distribution are assumed for the primary and secondary flows at the control-volume entrance (station 1), and a uniform, fully mixed flow is assumed at the exit of the control volume (station 3). No reaction is assumed to occur in the mixer, whereas a secondary combustion is considered in the ramjet burner if the primary flow is fuel rich or extra fuel is added in the ramjet burner. The condition at the ejector exit can be found when eight parameters are given [10]. The parameters to be defined are reduced by assuming the optimum condition [5,8] $p_{s,1} = p_{p,1}$. Moreover, when the flight Mach number M_0 and the altitude are given, all the secondary-flow properties (T_s^o , p_s^o , γ_s , and M_s) are known, whereas the primary-flow properties (T_p^o , γ_p , and M_p) are determined by the rocket-propellant mixture ratio for a given propellant combination. Thus, for a given flight condition and propellant combination, the characteristics of the mixed flow in station 3 are determined by four parameters, namely, the ejector geometry, that is, $\alpha = A/A^*$; the primary total pressure p_p^o , which determines $\beta = p_p^o/p_s^o$ and the primary rocket mass flow; the primary rocket mixture ratio φ , which determines the primary-flow characteristics, that is, γ_p , $\tau = T_p^o/T_s^o$, and $\nu = M_p/M_s$; the Mach number of the primary flow at station 1, $M_{p,1}$ (or alternately, the pressure at the mixer exit). Values of T_p^o , γ_p , and M_p are computed as a function of φ using CEA [11] and corresponding fourth-degree curve fits are embedded in the code.

First of all the following relations are defined:

$$\begin{aligned} f_0(\gamma, M) &= 1 + \frac{\gamma-1}{2}M^2; \quad f_1(\gamma, M) = [f_0(\gamma, M)]^{\frac{\gamma}{\gamma-1}} \\ f_2(\gamma, M) &= M\sqrt{\gamma f_0(\gamma, M)}; \quad f_3(\gamma, M) = 1 + \gamma M^2 \\ f_g(\gamma, M) &= \frac{\gamma\sqrt{M}}{[f_0(\gamma, M)]^{\frac{\gamma+1}{2(\gamma-1)}}}; \quad \varepsilon(\gamma, M) = \frac{1}{M} \left[\frac{2 + (\gamma-1)M^2}{\gamma+1} \right]^{\frac{\gamma+1}{2(\gamma-1)}} \\ B_1 &= \frac{\gamma_s-1}{\nu(\gamma_p-1)}; \quad B_2 = \frac{\gamma_p}{\gamma_s} B_1 \end{aligned}$$

The secondary-to-primary mass flow ratio μ can be evaluated

$$\begin{aligned} \mu &= \frac{\dot{m}_s}{\dot{m}_p} = \left(\frac{\alpha}{\varepsilon_1} - 1 \right) \sqrt{\frac{\tau f_2(\gamma_s, M_{s1})}{\nu f_2(\gamma_p, M_{p1})}} \\ &= \left(\frac{\alpha}{\varepsilon_1} - 1 \right) \sqrt{\frac{\tau f_g(\gamma_s, M_{s1})}{\nu \beta f_g(\gamma_p, M_{p1})}} \end{aligned} \quad (3)$$

where

$$\varepsilon_1 = \varepsilon(\gamma_p, M_{p1}) \quad \text{and} \quad M_{s1} = \sqrt{\frac{2}{\gamma_s-1} \left[\left(\frac{f_1(\gamma_p, M_{p1})}{\beta} \right)^{\frac{\gamma_s-1}{\gamma_s}} - 1 \right]} \quad (4)$$

The energy and continuity equations give the properties of the mixed flow

$$\begin{aligned} \gamma_3 &= \gamma_s \frac{\mu + B_2}{\mu + B_1}; \quad \tau_3 = \frac{T_3^o}{T_s^o} = \frac{\mu + B_2 \tau}{\mu + B_2} \\ \nu_3 &= \frac{M_3}{M_s} = \nu \frac{1 + \mu}{1 + \mu \nu} \end{aligned} \quad (5)$$

whereas, having combined momentum and continuity equations,

$$M_3^2 = \frac{(1-Z)\gamma_3 \pm \sqrt{(1-Z)\gamma_3^2 - Z\gamma_3}}{\gamma_3 - (1-Z)\gamma_3^2} \quad (6)$$

where

$$Z = 2 \frac{\tau_3/\tau}{\nu_3/\nu} (1 + \mu)^2 \left[\frac{\varepsilon_1 f_2(\gamma_p, M_{p1})}{\varepsilon_1 f_3(\gamma_p, M_{p1}) + (\alpha - \varepsilon_1) f_3(\gamma_s, M_{s1})} \right]^2 \quad (7)$$

Real roots are obtained for M_3 if $Z \leq \gamma_3/(\gamma_3 + 1)$. The negative sign root gives $M_3 < 1$, while the positive sign gives $M_3 > 1$. The subsonic solution is obtained also by allowing the possible supersonic solution to diffuse through a normal shock wave. When $Z < (\gamma_3 - 1)/\gamma_3$, the denominator is negative and only the subsonic solution exists because a negative numerator is required. The second law of thermodynamics is violated as Z approaches $(\gamma_3 - 1)/\gamma_3$ on the supersonic branch [9] (p_3^o would exceed the larger of the primary- and secondary-flow stagnation pressures). Both the roots give $M_3 = 1$ when $Z = \gamma_3/(\gamma_3 + 1)$: The ejector exit is choked. It is interesting to observe that the ejector can have a choked exit only if β is lower than a given value β_{M3} . In the present study only subsonic solutions are taken into account. Moreover, it is supposed that the mixer duct has a length which will allow a fully mixed flow at its end. Then the momentum equation allows one to compute the total pressure in station 3 and to determine the engine pressure ratio (EPR)

$$\begin{aligned} \text{EPR} = \frac{p_3^o}{p_s^o} &= \frac{f_1(\gamma_3, M_3)}{f_1(\gamma_s, M_{s1}) f_3(\gamma_3, M_3)} \left[\left(1 - \frac{\varepsilon_1}{\alpha} \right) f_3(\gamma_s, M_{s1}) \right. \\ &\quad \left. + \frac{\varepsilon_1}{\alpha} f_3(\gamma_p, M_{p1}) \right] \end{aligned} \quad (8)$$

B. Ejector Constraints and Operation

The ejector must face constraints that limit design parameters and performance. Three constraints concern the secondary-flow entrance into the ejector, one related to the aforementioned mixer exit choking ($M_3 \leq 1$), and another to the ramjet burner and one to the nozzle.

The following constraints must be satisfied at engine section 1:

1) Blockage: the primary flow should not occupy all of the mixer area, that is, $\alpha \geq \varepsilon(\gamma_p, M_{p1})$; then, for a given geometry α , an absolute maximum value of M_{p1} , $M_{p1,\text{lim}}$ exists.

2) Backflow: the static pressure p_{p1} should not exceed p_{s1}^o , that is, $\beta \leq f_1(\gamma_p, M_{p1})$; then, a maximum allowed value of β can be found: $\beta_{\text{max}}(\alpha, \gamma_p) = f_1(\gamma_p, M_{p1,\text{lim}})$.

3) Secondary-flow choking: $M_{s1} \leq 1$ and, assuming $p_{s1} = p_{p1}$, $\beta \geq f_1(\gamma_p, M_{p1})/f_1(\gamma_s, 1)$; then the limit for the secondary-flow's choking is $\beta_{\text{ck}}(\alpha, \gamma_p) = \beta_{\text{max}}/f_1(\gamma_s, 1)$.

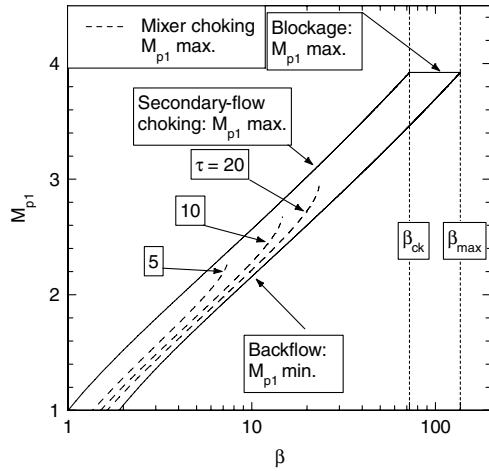


Fig. 2 Possible values of M_{p1} as a function of primary-to-secondary total pressure ratio β with $\alpha = 10$, $\gamma_p = \gamma_s = 1.4$, and $\nu = 1$.

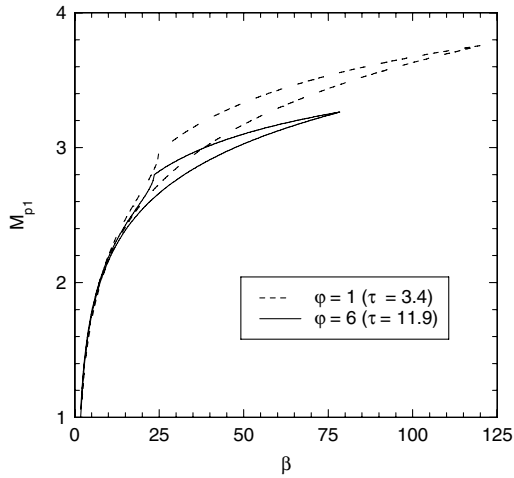


Fig. 3 Effects of rocket chamber mixture ratio ϕ on the ejector operation range at SLS conditions and $\alpha = 10$.

These constraints and the mixer exit choking limit ejector operation to a range of M_{p1} , bounded at each end as shown in Figs. 2 and 3. The lower limit of M_{p1} corresponds to the possible backflow of the primary flow. On other hand, the upper bound of M_{p1} is due to mixer exit choking if $1 \leq \beta \leq \beta_{M3}$ [being $\beta_{M3}(\alpha, \phi)$], secondary-flow choking in Eq. (1) if $\beta_{M3} < \beta \leq \beta_{ck}$, and blockage if $\beta_{ck} < \beta \leq \beta_{max}$. No ejector operation is possible if $\beta > \beta_{max}$. In the following a normalized index χ is introduced so that $\chi = 1$ for M_{p1} which determines the maximum values of μ , while $\chi = 0$ for the lower bound of M_{p1} . As far as the burner is concerned, a maximum given value of T_7^o is not to be exceeded, thus limiting the heating due to mixing and/or to secondary combustion. Finally, because it must be $p_e^o \geq p_0$, then, neglecting pressure losses in the ramjet burner and in the nozzle, $EPR f_1(\gamma_p, M_0) > 1$.

III. Evolutionary Algorithm

EAs begin with the random initialization of a population of individuals and do not require an initial guess of the solution. On the other hand, some working parameters allow one to control the evolution and the algorithm's capability of finding the optimal solution. The tuning of these parameters usually does not have a general validity and requires an additional computational cost. A cooperative evolutionary algorithm that synergistically joins the capabilities and peculiarities of genetic algorithms (GA), differential evolution (DE), and particle swarm optimization (PSO) has been developed [12] and has been used in this study to find the RBCC

engine's design parameters' combination which maximizes I_s while ensuring a minimum required T/A . An epsilon-constraint approach is used, penalizing solutions that do not have T/A greater than the required value or do not respect any other given constraints. The hybrid procedure basically runs the three different optimizers "in parallel"; the algorithms share the information concerning the best individuals found by each algorithm by using a cloning operator so that specific tuning of working parameters is not required. A new operator, called mass mutation, has also been introduced: A high percentage of individuals (usually over 90%) is eliminated when the mean distance between the individuals is smaller than a prescribed value and the optimal objective function is stuck on the same value for more than a prefixed number of iterations. In the following the three evolutionary optimizers used by the hybrid method and the information exchange procedure are described. See [13] for further details.

A. Genetic Algorithm

A starting population of N_i individuals is created randomly and evolution is performed just as in natural adaptation [14]. Each individual is characterized by the real values of N_p optimization variables. In the proposed algorithm, Bramlette's *extended random initialization* (ERI) [15] is introduced, whereby random initializations are tried for each individual until a significant solution is found or a maximum number of tries (e.g., 10) is reached. The initial effort in terms of computational cost is repaid with a faster convergence to the global optimum. The GA optimization tool here implemented can use three different types of *selection operators*, namely, the tournament selection, the roulette wheel selection, and the stochastic universal sampling. A *crossover operator* is then applied to get a new generation of individuals. Couples of individuals are randomly selected among the parent population so that each individual is chosen once. The crossover is applied parameter by parameter according to a probability distribution defined as

$$P(\psi) = \begin{cases} 0.5(\eta + 1)\psi^\eta & \text{for } \psi \leq 1 \\ 0.5(\eta + 1)/\psi^{(\eta+2)} & \text{otherwise} \end{cases} \quad (9)$$

For each parameter, the procedure determines the new values y_1 and y_2 from the values of the parent individuals x_1 and x_2 ; a random number $0 \leq u_r \leq 1$ is first chosen, ψ is determined so as $P(\psi) = u_r$ and the "children" are computed: $y_1 = 0.5[(x_1 + x_2) - \psi|x_2 - x_1|]$ and $y_2 = 0.5[(x_1 + x_2) + \psi|x_2 - x_1|]$. The parameter η controls how close the children solutions are with respect to the parent solutions (the larger η is, the closer the solutions are); $\eta = 2$ is usually suggested and this value is used in the following calculations. *Mutation* is applied to the new population to increase the number of explored solutions and keep diversity in the population. Some of the variables are changed, according to a small specified probability (here 2%). The new objective function for each of the new generation individual is finally evaluated. This procedure is repeated for a fixed N_g number of iterations or until a prefixed number of function evaluations is reached.

B. Differential Evolution

The differential evolution [16] is a parallel direct search method that uses a population of N_i individuals of N_p dimension for N_g generations, just as GA does. ERI can be optionally added as well. Basically, DE generates new vectors of parameters by adding the weighted difference between two population vectors to a third one. If the resulting individual provides a better objective function than a predetermined population member, in the following generation the new individual will replace the one with which it was compared; otherwise, the old individual will be retained. This basic principle can be varied: There are several practical variants of DE. In the present study the so-called DE/best/1 variant is used, that is, $y = x_{best} + F(x_1 - x_2)$, where F is a scaling factor (a constant $F = 0.6$ is assumed), x_1, x_2 are the variable values of vectors chosen randomly and x_{best} is the variable value of the best individual in the population. The crossover probability is fixed at 0.8.

C. Particle Swarm Optimization

PSO is a population based stochastic optimization technique [17], inspired by social behavior of bird flocking or fish schooling. Compared to GA, PSO is quite easy to implement and there are a few parameters to adjust. A population of potential solutions is randomly generated and the procedure searches for optima by updating generations, but unlike GA or DE, PSO has no operators such as crossover and mutation. The values of the N_p optimization variables define the position of each solution, called particle, in the problem space. A velocity vector that rules the motion of the particle is also introduced. The particles fly through the problem space by following the particle with the best fitness function. In every iteration, each particle moves according to its instantaneous velocity, which is updated by the following two criteria: The velocity is changed in order to move the particle toward the best solution P_{best} reached so far by the particle itself and toward the best solution G_{best} reached so far by the whole population. The particle updates its velocity and position according to the relations $v = v + c_1 \cdot k_1 \cdot (x_{P_{\text{best}}} - x) + c_2 \cdot k_2 \cdot (x_{G_{\text{best}}} - x)$ and $y = x + v$, where v is the particle velocity, x and y are the current and updated particle positions, k_1, k_2 are random numbers between (0,1). c_1, c_2 are learning factors (usually $c_1 = c_2 = 2$). Different strategies can be used: Trelea's type 1 is used in the present study [18]. Compared with GAs and DE, the information sharing mechanism in PSO is significantly different. In GAs and DE, individuals share information with each other, whereas in PSO, only G_{best} shares the information with each others: The evolution only looks for the best solution.

D. Information Exchange Procedure

In standard multipopulation optimization algorithms, a certain number of subpopulations evolves independently and, from time to time, an operator called *migration* performs an exchange of information. The amount of migration of individuals and the pattern of that migration determines how much genetic diversity can occur. The use of migration sometimes is not efficient for a multi-optimizer algorithm, because convergence can be delayed if we move optimal information from a good-working optimizer to a weak one that might not be able to take it to convergence. Moreover, migrating randomly chosen individuals might not be so convenient, because good information can be trapped in badly optimized populations and not passed to good ones. In our hybrid algorithm another operator, called *cloning*, just "clones" the best ones and inserts them into the other subpopulations, instead of moving individuals from a subpopulation to another like migration does. Ring, neighborhood, and complete web strategy are the cloning patterns here implemented.

IV. Numerical Results

Liquid-oxygen/liquid-hydrogen primary rocket and sea-level-static (SLS) flight conditions are considered. If fuel is added in the ramjet burner (AB engine), then the design parameters vector is $\mathbf{x} = (\alpha, \beta, \varphi, \chi, \delta)$; otherwise $\delta = 0$ (dry engine), and $\mathbf{x} = (\alpha, \beta, \varphi, \chi)$. The following bounds are considered: $1 \leq \varphi \leq 10$, $p_p^o \leq 100$ bar (open cycle feeding system), $T_g^o \leq 2000$ K, and, to reduce the ejector's mixing length, $\alpha/\varepsilon_1 \leq 50$ and $\alpha \leq 500$. As said before, the synergistic use of different optimizers does not require the optimization of the working parameters for each simple algorithm: the same standard set of working parameters and strategies is used for both dry and AB engine problems, but the population size for GA, that is more sensitive to the problem's number of variables, and the maximum number of the function evaluation, the AB engine problem has one extra parameter. Three subpopulations (100 individuals for

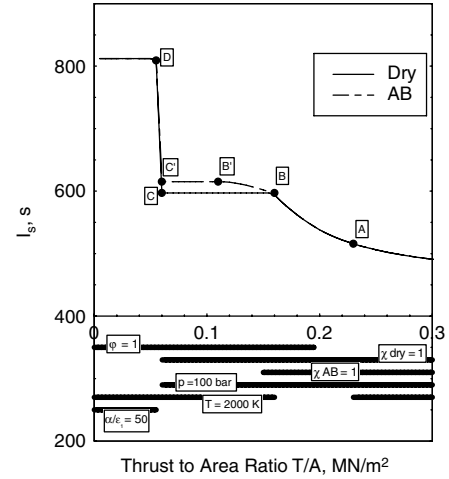


Fig. 4 Objective function values of the ERR design: dry and AB engine with $p_p^o \leq 100$ bar and $1 \leq \varphi \leq 10$ at SLS conditions.

GA/dry engine, 200 for GA/AB engine, 60 for DE, and 30 for PSO) have been allowed to evolve until the maximum number (38,000 for the dry engine, 58,000 for the AB engine) for the function evaluation has been reached. Mass mutation is performed every 50 stuck iterations, and the passage of six individuals between subpopulations happens every 20 iterations. In Table 1 results of a statistical study on the behavior of the hybrid algorithm is presented, considering the more costly case of the AB engine. The optimizer ran 40 times for three different thrust to area ratios, and the efficiency (number of times the minimum value has been reached in percentage with a precision of 0.001) is evaluated.

The efficiency is always over 90% for all the cases, showing that evolutionary algorithms are suitable for this kind of parametric problem, and that the standard set of working parameters adopted is reliable and allows great savings in terms of computational cost. A more complete set of results is shown in Figs. 4–6 for open cycle feed systems ($p_p^o \leq 100$ bar) and $1 \leq \varphi \leq 10$. Figure 4 shows the objective functions; in the lower part of the same figure, continuous lines are drawn when the solution is located on the contour of the admissible region (labels indicate the related active bounds). Figure 5 shows the optimal values of the design parameters and Fig. 6 shows main ejector performance parameters including $w_{\text{lim}} = \sqrt{2c_{pe} T_g^o}$. The dry engine solution is optimal for most of the analyzed T/A range. If high values of T/A are required, the mixer exit is choked. When lowering the required T/A , I_s is augmented by increasing the air mass involved: Looking at Figs. 5 and 6 one can see that the engine is enlarged and μ is increased, while w_e and EPR decrease. The maximum allowable p_p^o and T_g^o are used until point A is reached. For lower values of T/A , it is convenient to exploit lighter combustion gases, even if T_g^o is reduced: The equivalence ratio Φ , shown in Fig. 6, has a larger increment due to the steeper descent of the primary mixture ratio, until the lower bound $\varphi = 1$ is reached. Then again T_g^o is increased up to the upper bound 2000 K, thus obtaining solution B. If the dry engine is considered, solution B remains the best one down to T/A values corresponding to solution C. The mixer exit is nearly choked. Then, due to the low T/A values required, the Pareto optimal solution jumps to the contour dictated by the mixer area constraints: Even if $\varphi = 1$, an oxidizer-rich secondary combustion occurs ($\Phi < 1$), due to the high value of μ . It is interesting to note that, in this case, the solutions require an unchoked mixer exit ($\chi < 1$). When fuel injection in the ramjet burner is

Table 1 Optimization method performance for the AB engine

T/A	Min. value	Mean value	Std dev V	Efficiency	NFE_{min}	NFE_{mean}	Std dev N
0.1	615.0529175	615.0522888	$9.94E-05$	95.0%	42,485	52,938	4399.26
0.2	538.197937	538.197937	$3.60E-14$	100.0%	30,845	44,078	3875.86
0.3	491.0453491	491.045295	$8.56E-06$	97.5%	39,866	52,304	3892.87

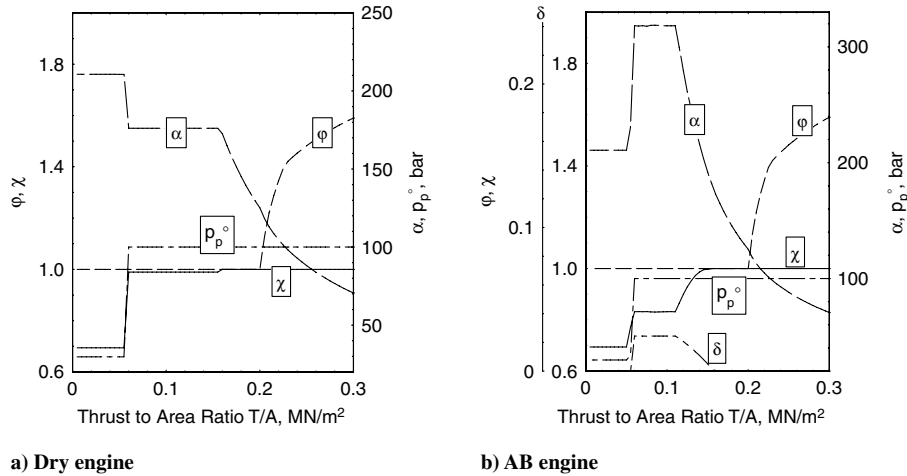


Fig. 5 Design parameters values with $p_p^o \leq 100$ bar and $1 \leq \phi \leq 10$ at SLS conditions.

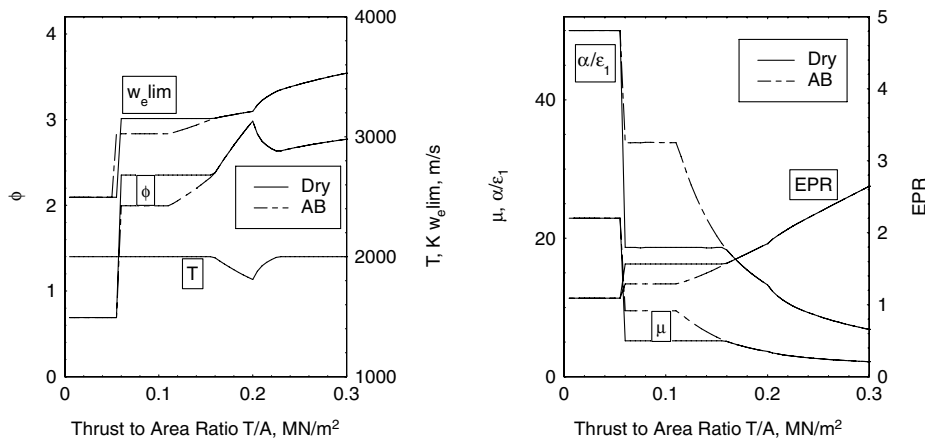


Fig. 6 Ejector performance parameters with $p_p^o \leq 100$ bar and $1 \leq \phi \leq 10$ at SLS conditions.

considered, then T_7^o can be kept on its upper 2000 K limit with a larger μ and an unchoked mixer exit: An extension from B to B' is possible, allowing higher I_s . Then, as for the dry engine, there is a T/A range where, before jumping to D-like solutions, the B' solution is the best. Higher performance can be obtained by using a closed cycle feeding system, thus allowing for higher p_p^o .

V. Conclusions

In the present study a multi-objective design optimization of a rocket based combined engine has been performed. Objective functions are specific impulse and thrust to area ratio. To have a reasonable computation time, a control-volume approach is used to evaluate the engine performance. Propellant combination effects and ejector operation constraints are taken into account. The corresponding multi-objective optimization problem is solved by using a hybrid evolutionary algorithm, which employs synergistically a genetic algorithm, differential evolution, and particle swarm optimization. Thanks to the information sharing between the basic algorithms, achieved by cloning the best individuals at prescribed intervals, it is possible to obtain the optimal set of design parameters with an excellent efficiency and low computational cost. To demonstrate the feasibility of the present approach, sea-level-static flight conditions and a liquid-oxygen/liquid-hydrogen primary rocket have been considered, taking into account the present technological limits. Values of objective functions, ejector performance, and engine design parameters are shown. Solutions are presented highlighting the effects of the design parameters' bounds and of the considered constraints.

Acknowledgment

The financial support of Regione Piemonte is gratefully acknowledged.

References

- [1] Heiser, W. H., and Pratt, D. T., *Hypersonic Airbreathing Propulsion*, AIAA Education Series, AIAA, Washington, D.C., 1994, pp. 446–452.
- [2] Etele, J., Parent, B., and Sislian, J. P., "Analysis of Increased Compression Through Area Constriction on Ejector-Rocket Performance," *Journal of Spacecraft and Rockets*, Vol. 44, No. 2, 2007, pp. 355–364. doi:10.2514/1.26915
- [3] Dutton, J., and Carroll, B., "Optimal Supersonic Ejector Designs," *Journal of Fluids Engineering*, Vol. 108, 1986, pp. 414–420.
- [4] Dutton, J. C., and Carroll, B. F., "Limitation of Ejector Performance due to Exit Choking," *Journal of Fluids Engineering*, Vol. 110, No. 10, 1988, pp. 91–93.
- [5] Han, S., Peddieson, J., and Gregory, D., Jr., "Ejector Primary Flow Molecular Weight Effects in an Ejector-Ram Rocket Engine," *Journal of Propulsion and Power*, Vol. 18, No. 3, 2002, pp. 592–599. doi:10.2514/2.5973
- [6] Alperin, M., and Wu, J.-J., "Thrust Augmenting Ejectors, Part 1," *AIAA Journal*, Vol. 21, No. 10, 1983, pp. 1428–1436. doi:10.2514/3.60148
- [7] Jahingir, N. M., and Huque, Z., "Design Optimization of Rocket-Based Combined-Cycle Inlet/Ejector System," *Journal of Propulsion and Power*, Vol. 21, No. 4, 2005, pp. 650–655. doi:10.2514/1.10788
- [8] Fabri, J., and Siestruncun, R., "Supersonic Air Ejectors," *Advances in Applied Mechanics*, Vol. 5, Academic Press, New York, 1958, pp. 1–34.
- [9] Emanuel, G., "Comparison of One-Dimensional Solutions with

- Fabri Theory for Ejectors" *Acta Mechanica*, Vol. 44, Nos. 3–4, 1982, pp. 187–200.
doi:10.1007/BF01303337
- [10] Dutton, J. C., Mikkelsen, C. D., and Addy, A. L., "A Theoretical and Experimental Investigation of the Constant Area, Supersonic-Supersonic Ejector," *AIAA Journal*, Vol. 20, No. 10, 1982, pp. 1392–1400.
doi:10.2514/3.51199
- [11] Gordon, S., and McBride, B. J., "Computer Program for Calculation of Complex Chemical Equilibrium Compositions and Applications," NASA RP-1311, 1994.
- [12] Rosa Sentinella, M., "Development of New Procedures and Hybrid Algorithms for Space Trajectories Optimization," Ph.D. Thesis, Politecnico di Torino, Turin, Italy, April 2008.
- [13] Rosa Sentinella, M., and Casalino, L., "Hybrid Evolutionary Algorithm for the Optimization of Interplanetary Trajectories," *Journal of Spacecraft and Rockets*, Vol. 46, No. 2, 2009, pp. 365–372.
doi:10.2514/1.38440
- [14] Goldberg, D. E., *Genetic Algorithms in Engineering Design*, Wiley, New York, 1997.
- [15] Bramlette, M. F., "Initialization, Mutation, and Selection Methods in Genetic Algorithms for Function Optimization," *Proceedings of the Fourth International Conference on Genetic Algorithms*, edited by R. K. Belew, and L. B. Booker, Morgan Kaufmann, San Mateo, CA, July 1991, pp. 100–107.
- [16] Storn, R., "On the Usage of Differential Evolution for Function Optimization," *1996 Biennial Conference of the North American Fuzzy Information Processing Society*, North American Fuzzy Information Processing Society, Berkeley, CA, 1996, pp. 519–523.
- [17] Kennedy, J., and Eberhart, R. C., "Particle Swarm Optimization," *Proceedings of the IEEE International Conference on Neural Networks*, IEEE, Piscataway, NJ, 1995, pp. 1942–1948.
- [18] Trelea, I. C., "The Particle Swarm Optimisation Algorithm. Convergence, Analysis and Parameter Selection," *Information Processing Letters*, Vol. 85, No. 6, 2003, pp. 317–325.
doi:10.1016/S0020-0190(02)00447-7

C. Segal
Associate Editor